A Novel Conductivity Composite Based on Polyaniline/Zirconium Phenylphosphonate

Changhua Liu, Lina Zhu, Haixia Wu, Yajuan Yang

College of Chemistry and Chemical Engineering, Southwest University, 400715, Chongqing, People's Republic of China

Received 26 September 2009; accepted 17 June 2010
DOI 10.1002/app.32968
Published online 30 August 2010 in Wiley Online Library (wileyonlinelibrary.com).

ABSTRACT: A novel conductivity composite from polyaniline (PANI) and layered zirconium phenylphosphonate (ZrPP) was carried out through *in situ* chemical oxidation polymerization by the addition of an appropriate amount of ammonium peroxodisulfate solution, and the relevant structure and properties were investigated. The composites were characterized by Fourier transform infrared spectroscopy, X-ray diffraction, and scanning electron microscopy. The electrical conductivity was measured by the four-probe technique. The electrical conductivity of the composites improved with increasing ZrPP loading, and the materials had reasonably good electrical properties, even with 40 wt % loadings of ZrPP in the polymer matrix. The results reveal that π–π interaction was formed in the composites, which enhanced the electrical conductivity of the composites compared to that in neat PANI. © 2010 Wiley Periodicals, Inc. J Appl Polym Sci 119: 2334–2338, 2011

Key words: conducting; polymers; FTIR; nanocomposites; structure–property relations; X-ray

INTRODUCTION

Since intrinsically conducting polymers were discovered in 1960, they have become an attractive research subject because of their interesting properties and numerous applications.[1] Among the available intrinsically conducting polymers, polyaniline (PANI) is one of the most excellent candidates, and it has been found to be the most promising compared to other intrinsically conducting polymers. PANI has many special advantages in the field of conducting polymers for many reasons, including its relatively low cost, simple polymerization methods, high yield of polymerization product,[2] unique doping mechanisms, relatively high electrical conductivity, and perfect environmental stability.[3,4] On the basis of the previously mentioned advantages, according to the literature, there are two main applications for PANI. First, PANI as an electrolyte membrane is used in direct methanol fuel cells. The PANI electrolyte membrane in direct methanol fuel cells not only conducts protons but also serves as barrier for methanol.[5–7] Second, PANI can be used as a conductive material; it has potential applications in electrochemical sensors,[8,9] antioxidants,[10,11] and so on. However, the main problem associated with the effective utilization of PANI is inherent in its lower level of conductivity compared to metal and its infusibility and poor solubility in all available solvents.[12,13] Therefore, there is ample scope for modifying the conductivity and processability of PANI through the selection of a suitable dopant and a suitable level of doping and also through the control of its structure during synthesis.[14,15] Among these modifications, layered compound/PANI nanocomposites have shown extraordinary promise as high-performance materials because they possess better properties and more applications than PANI. A large number of layered materials, including montmorillonite and α-zirconium phosphate (α-ZrP), have been studied as composite materials for PANI and have already proven to effective in improving the electrical properties of PANI.[16,17] Compared to natural montmorillonite clay, α-ZrP exhibits several additional advantages, including a much higher purity and ion-exchange capacity, an easier process of intercalation, and a manipulated surface functionality.[18–20] Thus, α-ZrP is one of the most extensively used layered phosphates.[21,22] On the basis of the manipulated surface functionality, it was interest to us that phenylic ring groups were projected into the interlayer region instead of —OH [namely, zirconium phenylphosphonate (ZrPP)]. We supposed that because of the presence of ZrPP, the phenylic rings possess many π electrons and that this increases the number of carriers, which accelerate the movement of electrons in the PANI chains.

From this analysis, in this study, we prepared PANI/ZrPP composites through chemical oxidation

Correspondence to: C. Liu (chliu@swu.edu.cn).

polymerization. The structure and properties were studied by X-ray diffraction (XRD), Fourier transform infrared (FTIR) spectroscopy, scanning electron microscopy (SEM), and electrical conductivity measurements. The influence of phenylic ring groups on the electrical conductivity was also examined.

EXPERIMENTAL

Chemicals and instruments

The monomer aniline was purchased from Chongqing Chuandong Chemical Reagent Factory (Chongqing, China) and was distilled before use. Zirconium oxychloride octahydrate ($ZrOCl_2 \cdot 8H_2O$; 99%) was purchased from Tianjin Kermel Chemical Reagent Development Center (Tianjin, China). Phenylphosphonic acid and hydrofluoric acid were purchased from Chongqing Beibei Chemical Reagent Factory (Chongqing, China). Ammonium peroxodisulfate [APS; $(NH_4)_2S_2O_8$; 98%] was purchased from Chongqing Taixin Chemical Reagent Factory (Chongqing, China). FTIR spectroscopy of the composites were recorded with a Nicolet 170SX FTIR spectrometer (Madison, WI) in the wavelength range of 4000–500 cm^{-1} in the attenuated total reflection mode. XRD patterns of the samples were carried out with a XRD-3D, PuXi X-ray diffractometer (Beijing, China) under the following conditions: nickel-filtered Cu Kα radiation ($\lambda = 0.15406$ nm) at a voltage of 36 kV and a current of 20 mA. The scanning rate was 4°/min in the angular range of 3–50° (2θ). The SEM micrograph was obtained on a scanning electron microscope (S-4800, Hitachi, Tokyo, Japan) to determine the morphologies at an accelerating voltage of 5 kV. The room temperature conductivity was measured by a standard four-probe method with a Keithley 797A instrument (Shanghai, China). The samples were pelletized to a diameter of 1.3 cm and a thickness of 1.2 mm with a vacuum press at 8 MPa for 5 min.

Synthesis of ZrPP

ZrPP was synthesized as described in a previous study with slight modification, as follows[23]: A solution was obtained by the addition of 1.0 mol/L phenylphosphonic acid into a mixture solution containing hydrated zirconium oxychloride and concentrated hydrofluoric acid solution, which was made of 2/1 (the molar ratio) $C_6H_5PO(OH)_2/Zr^{4+}$ and a definite molar ratio of F^-/Zr^{4+}. No precipitation occurred at this point because the zirconium was present as the fluoro complex. We formed the precipitate slowly by heating at 70°C and kept it at this temperature for several days, periodically adding water to the system to maintain the constant volume of the solution. Finally, this precipitate was filtered off and air-dried. The chemical equations for the synthesis of ZrPP are shown as follows:

$$ZrO^{2+} + 6HF \longrightarrow ZrF_6^{2-} + H_2O + 4H^+ \quad (1)$$

$$ZrF_6^{2-} \xrightarrow{\Delta} Zr^{4+} + 6F^- \quad (2)$$

$$Zr^{4+} + 2H_2O_3PC_6H_5 \rightarrow Zr(H_2O_3PC_6H_5)_2 + 4H^+ \quad (3)$$

Synthesis of neat PANI

A definite amount of aniline was mixed with 10 mL of distilled water and was added dropwise to a 1*M* HCl solution, and then, APS as an oxidant was added to this solution to polymerize aniline. The molar ratio of monomer to oxidant was kept at 1 : 1, and the reaction temperature was kept at 0–5°C for 24 h.

Synthesis of the PANI/ZrPP composites

An amount of 1 g of ZrPP was dispersed in an aqueous solution system, with acetone added to the dispersion system to help dissolve it. The resulting dispersion was followed by 2 h of ultrasonic treatment. A definite amount of aniline was mixed with 10 mL of distilled water, and the aniline was dropped to the dispersed ZrPP system dropwise. Then, a 1*M* HCl solution was added to this system, and APS as an oxidant was added to the mixture solution to polymerize aniline. The polymerization temperature was kept at 0–5°C for 24 h; the molar ratio of monomer to oxidant was kept at 1 : 1. For comparison, PANI/ZrP was prepared through the same fabrication process.

RESULTS AND DISCUSSION

X-ray diffractometry

Figure 1 shows the XRD patterns of ZrPP, neat PANI, and a series of PANI/ZrPP composites with different loading levels of ZrPP. The XRD pattern for ZrPP [Fig. 1(a)] exhibited an intense peak, with the characteristic (002) reflection at a low angle related to the lamellar solids. The interlayer distance in the (002) direction was estimated from Bragg's law ($2d \sin\theta = \lambda$), and the *d*-spacing was 15.2 Å, which corresponded to this diffraction for ZrPP, the value observed in the literature.[24,25] For PANI [Fig. 1(b)], there was a crystallite, whose sharp peak was at $2\theta = 25°$ in the angle from 5° to 50°, which was similar to other results of PANI.[26] When the XRD patterns of neat PANI and ZrPP were compared with those of the PANI/ZrPP composites, the characteristic peaks for PANI and ZrPP could be found; it was clear that the characteristic peak of the

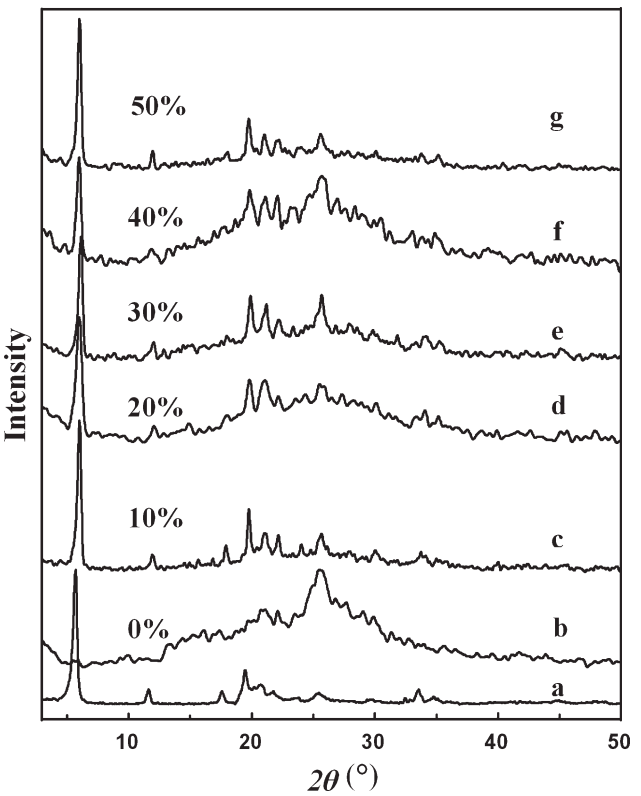

Figure 1 XRD patterns of (a) ZrPP, (b) neat PANI, and (c–g) PANI/ZrPP composites with different ZrPP loadings.

PANI/ZrPP composites [Fig. 1(c–g)] was a combination of ZrPP and PANI, and the interlayer spacing of the layered ZrPP remained constant. This showed the polymerization outside the interlayer of the crystalline ZrPP. A possible reason was that hydrochloric acid intercalated into ZrPP during the treatment of aniline at the presence of hydrochloric acid; because hydrochloric acid was a strong electrolyte, hydrogen ions were quickly spread to the layer of ZrPP and formed aniline hydrochloride. There was strong competition between ion-exchange reactions in the intercalated aniline and polymerization reaction with APS. The results indicate that the formation of composites resulted in a physical composite. As shown in Figure 1, the intensity of the characteristic peaks of ZrPP in the composites decreased with increasing ZrPP loading [Fig. 1(c–f)]; when the loading of ZrPP was at 40 wt %, compared to the other curves, the intensity of the characteristic peak of ZrPP was the weakest, as shown in Figure 1(f). This suggested that the polymer and fillers were complexing, preferably when ZrPP was dispersed well in PANI at a 40% loading. This indicated that there was interaction between the polymer and fillers. The characteristic peak of ZrPP became stronger when the ZrPP loading was 50% [Fig. 1(g)]. This suggested that fillers were reunited and could not be dispersed well in PANI, which influenced the interaction between the polymer and fillers. These results were also confirmed by the FTIR results.

FTIR analysis

The FTIR spectra of the layered ZrPP, PANI/ZrPP composites, and neat PANI are shown in Figure 2 from 1600 to 650 cm^{-1}. For the FTIR spectrum of ZrPP [Fig. 2(a)], the presence of bands at 693, 728, 748, and 1438 cm^{-1} was an indication of the presence of phenylic groups in the ZrPP framework, and PO_3 vibrations were observed in the range 1163–1039 cm^{-1}, along with the C—P vibration at 1160 cm^{-1}; this was similar to a previous report.[23] For the FTIR spectrum of PANI [Fig. 2(g)], the characteristic peaks at 1474 and 1567 cm^{-1} were assigned to the C=C stretching modes of the benzenoid ring and the quinoid ring,[27] respectively, which indicated the oxidation state of PANI (emeraldine salt). As is commonly observed for emeraldine salts, the benzenoid band at 1474 cm^{-1} was more intense than that of the quinoid band at 1567 cm^{-1}. The peak at 1300 cm^{-1} corresponded to the C—N stretching vibration of the secondary aromatic amine.[28] The peak at 1112 cm^{-1} was due to the C—H in-plane bending mode of

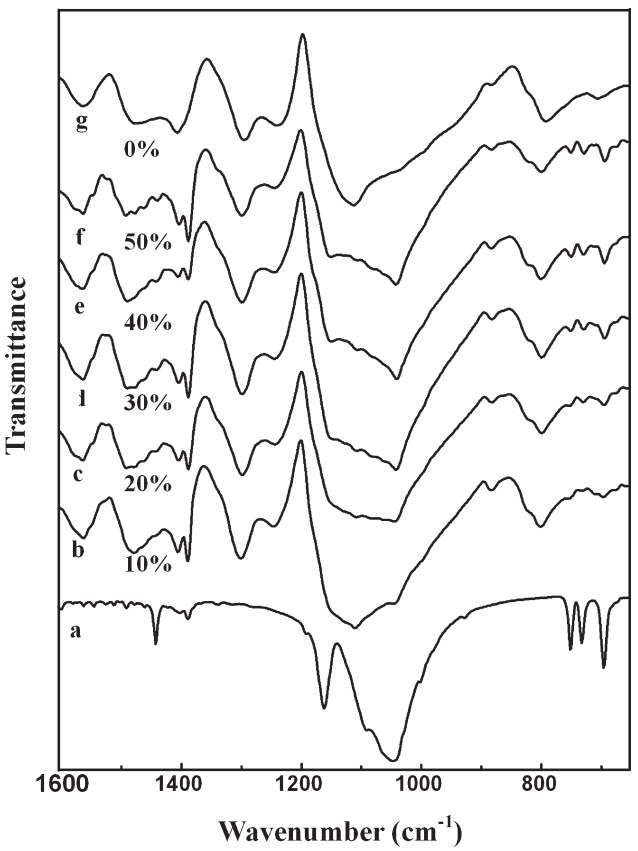

Figure 2 FTIR spectra of (a) ZrPP, (g) neat PANI, and (b–f) PANI/ZrPP composites with different ZrPP loadings.

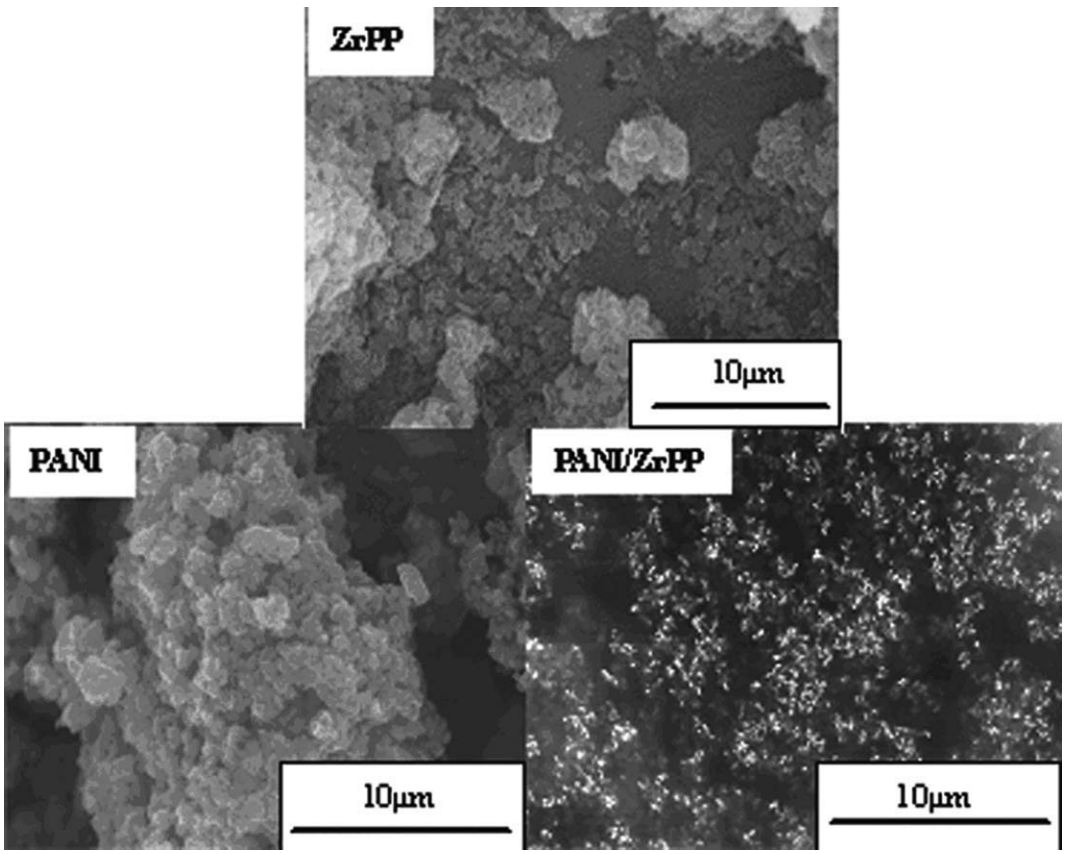

Figure 3 SEM micrographs of ZrPP, PANI, and the PANI/ZrPP composite (40% ZrPP loading).

permigraniline.[29] These results were in agreement with those in a previous report for PANI. When we compared the spectra of the PANI/ZrPP composites with those of neat PANI and ZrPP, the vibration bands assigned to the characteristic bands for PANI and ZrPP were found, as shown in Figure 2(b–f). The PANI/ZrPP composites showed nearly identical wave numbers and the peak positions of the main IR bands. However, there were several differences between the FTIR spectra of the PANI/ZrPP composites and that of PANI. The spectra of the PANI/ZrPP composites showed an inverse intensity ratio of the bands at 1567 and 1474 cm^{-1}, compared with those peaks of PANI. These data revealed that the PANI in the composites was richer in the quinoid unit than the neat PANI. This also suggested that the π-bonded surface of the ZrPP might have interacted strongly with the conjugated structure of PANI, especially through the quinoid ring.[30] In addition, changes in the FTIR spectra were observed with the increase of ZrPP loading. It was obvious that the peak at 1112 cm^{-1} in PANI shifted to a lower wave number in the PANI/ZrPP composites, and other peaks changed slightly. The peaks at 1157 and 1042 cm^{-1} in ZrPP shifted to 1146 and 1037 cm^{-1}, respectively, in the PANI/ZrPP composites. These changes indicated that van der Waals interactions between ZrPP and PANI formed, which resulted in the π–π interaction between PANI and the phenylic ring of ZrPP.

Morphology

The SEM micrographs of ZrPP, PANI, and PANI/ZrPP (40% ZrPP loading) are displayed in Figure 3. The ZrPP crystal clearly showed a layered structure. Neat PANI exhibited particle agglomeration. The SEM micrograph of the PANI/ZrPP composite was different because of the presence of the ZrPP. When PANI/ZrPP was compared with ZrPP and neat PANI, as shown in Figure 3, it was clear that polymer composites formed, along with some granular structure, and that the particle size decreased. This confirmed the homogeneous distribution of ZrPP in PANI. Thus, the microstructure and loading of ZrPP had a great influence on the modification of PANI. The presence of ZrPP at different loadings enhanced the conductivity of the host polymer when the ZrPP loading was no more than 40% (refer to the Electrical Conductivity section).

Electrical conductivity

The measurement of the electrical conductivity of PANI/ZrPP in contrast to that of neat PANI is shown in Table I Unlike neat PANI, the electrical

TABLE I
Conductivity Values of the Pure PANI and Nanocomposites at Room Temperature

Content (ZrPP %)	Conductivity (S/cm)
0	3.828×10^{-4}
10	0.811
20	1.136
30	1.313
40	1.625
50	0.938

conductivity of the PANI/ZrPP composites depended on the properties of both the host PANI and the guest ZrPP. As is shown clearly in Table I, when these systems were exposed to the addition of ZrPP, there was an obvious increase in the electrical conductivity with the addition of 40 wt % ZrPP; it increased by four orders of magnitude (1.625 S/cm) compared to that of neat PANI (3.828×10^{-4} S/cm). The electrical conductivity of the 40 wt % ZrPP composites was 4245 times higher than that of neat PANI. Compared with the electrical conductivity of the PANI/ZrP composites (1.236×10^{-3} S/cm at 40% ZrP loading), the electrical conductivity of ZrPP/PANI increased by three orders of magnitude. A possible reason was that the phenylic ring of ZrPP and PANI produced a weak electric field. ZrPP increased the overlapping degree of the π electron cloud in the PANI molecules' conjugate plane, and the phenylic ring, which stretched the internal layer, increased the density of the π electron. There were π–π interactions from the surface of the ZrPP and the quinoid ring of PANI molecular chains under such an environment. Simultaneously, ZrPP increased the number of π electron in the presence of the phenylic ring; this was equal to the increase in the number of carriers, which accelerated π–π electron transition in the PANI chains and reduced the electrical conductance activation energy in a certain range. The results led to a faster transferable speed of electrons on the molecular PANI chains and improved the degree of electron delocation between the two components, which resulted in an increase in the electrical conductivity. However, when the loading of ZrPP was added to 50 wt %, the electrical conductivity reduced to 0.938 S/cm. A possible reason was that there was an agglomeration of fillers in this system that could not disperse well in PANI, which blocked the speed of π electrons in the PANI chains. These conclusions were consistent with the previous discussion.

CONCLUSIONS

In this study, the preparation of PANI/ZrPP composites was successfully achieved with the technique of *in situ* chemical oxidation polymerization. The composites were characterized by FTIR spectroscopy, XRD, and SEM. The results reveal that the dropping ZrPP was homogeneously dispersed in the PANI matrix and π–π interactions were formed in the composite. The presence of ZrPP in the matrix had a greater influence on the conductivity values than that of PANI. The conductivity increased with the loading of ZrPP, which had the highest value at the 40% ZrPP loading, and resulted in π–π interactions between PANI and the phenylic ring of ZrPP.

References

1. Bhadra, S.; Khastgir, D.; Singha, N. K.; Lee, J. H. Prog Polym Sci 2009, 34, 783.
2. Martins, C. R.; Freitas, P. S.; Paoli, M. A. Polym Bull 2003, 49, 379.
3. Li, X. G.; Huang, M. R.; Lu, Y. Q.; Zhu, M. F. J Mater Chem 2005, 15, 1343.
4. Wei, Y.; Hariharan, R.; Patel, S. A. Macromolecules 1990, 23, 758, and references therein.
5. Chen, C. Y.; Garnica-Rodriguez, J. I.; Duke, M. C.; Dalla Costa, R. F.; Dicks, A. L.; Diniz da Costa, J. C. J Power Sources 2007, 166, 324.
6. Yang, Z. W.; Coutinho, D. H.; Sulfstede, R.; Balkus, K. J.; Ferraris, J. R. J Membr Sci 2008, 313, 86.
7. Nagarale, R. K.; Gohil, G. S.; Shahi, V. K. J Membr Sci 2006, 280, 389.
8. Dhaoui, W.; Bouzitoun, M.; Zarrouk, K.; Ben Ouada, H.; Pron, A. Synth Met 2008, 158, 722.
9. Li, X.; Ju, M.; Li, X. Sens Actuator B 2004, 97, 144.
10. Gizdavic-Nikolaidis, M.; Travas-Sejdic, J.; Kilmartin, P. A.; Bowmaker, G. A.; Cooney, R. P. Curr Appl Phys 2004, 4, 343.
11. Kilmartin, P. A.; Gizadavic-Nikolaidis, M.; Zujovic, Z.; Travas-Sejdic, J.; Bowmaker, G. A.; Cooney, R. P. Synth Met 2005, 153, 153.
12. Cho, M. S.; Park, S. Y.; Hwng, J. Y.; Choi, H. J. Mater Sci Eng C 2004, 24, 15.
13. Rao, P. S.; Subrahmanva, S.; Sathyanarayana, D. N. Synth Met 2003, 139, 397.
14. Bhada, S.; Chattopadhyay, S.; Singha, N. K. J Appl Polym Sci 2008, 108, 57.
15. Bhadra, S.; Singha, N. K.; Khastgir, D. Synth Met 2006, 156, 1148.
16. Olad, A.; Rashidzadeh, A. Prog Org Coating 2008, 62, 293.
17. De, S. K.; De, A.; Das, A. Mater Chem Phys 2005, 91, 477.
18. Clearfield, A.; Berman, J. R. J Inorg Nucl Chem 1981, 43, 2141.
19. Clearfield, A.; Duax, W. L.; Garces, J. M.; Medina, A. S. J Inorg Nucl Chem 1972, 34, 329.
20. Sun, L.; Boo, W. J.; Browning, R. L.; Sue, H. J.; Clearfield, A. Chem Mater 2005, 17, 5606.
21. Clearfield, A.; Smith, G. Inorg Chem 1969, 8, 431.
22. Sue, H. J.; Gam, K. T.; Bestaoui, N.; Clearfield, A.; Miyamoto, M.; Miyatake, N. Acta Mater 2004, 52, 2239.
23. Vanusa, S. O.; Ruiz, A. C. Thermochim Acta 2004, 420, 73.
24. Scott, K. J.; Zhang, Y.; Wang, R.; Clearfield, A. Chem Mater 1995, 7, 1095.
25. Alberti, G.; Costantino, U.; Allulli, S.; Tomassini, N. J. Inorg Nucl Chem 1978, 40, 1113.
26. Amrithesh, M.; Aravind, S.; Jayalekshmi, S.; Jayasree, R. S. J Alloys Compd 2008, 458, 523.
27. Cataldo, F.; Maltese, P. Eur Polym J 2002, 38, 1791.
28. Tursun, A.; Zhang, X. G.; Ruxangul, J Mater Chem Phys 2005, 90, 367.
29. Lei, Z. B.; Zhang, H. C.; Ma, S. H.; Ke, Y. X.; Li, J. M.; Li, F. Q. Chem Commun 2002, 7, 676.
30. Quillard, S.; Louarn, G.; Lefrant, S.; MacDiarmid, A. G. Phys Rev B 1994, 50, 12496.